Available online at www.sciencedirect.com
ScienceDirect
International Journal of Thermal Sciences 46 (2007) 802–811
International Journal of Thermal Sciences
www.elsevier.com/locate/ijts

Statistical dynamic features of sludge drying systems

Li He Chai *

Associate professor, School of Environmental Science and Engineering, Tianjin University, Tianjin 300072, China

Received 28 March 2006; received in revised form 14 October 2006; accepted 19 October 2006

Available online 17 November 2006

Abstract

The drying of sludge has become an important procedure for sludge disposal. Although many studies on the drying of sludge have been carried out recently, little attention was paid to the internal dynamics of dried sludge, which largely influenced phenomenal drying process. This paper proposed a statistical dynamic framework to analyze the physical mechanisms of sludge drying process. Based on the new method, the fractal dimension of a drying structure was derived analytically and its relationship with some controlling factors was analyzed. Experiments were performed to validate the theoretical analyses and good agreement was found. Not only provides a reasonable mechanistic description of internal structures of drying sludge, this work is of help to many industrial applications.

Keywords: Sludge drying; Statistical; Dynamic; Fractal

1. Introduction

With rapid worldwide economic developments and increasing environmental concerns globally, wastewater treatment has become an important issue during past decades. This results a rapidly increased production of sludge from wastewater treatment plants [1,2]. Problems associated with sludge treatments have attracted much attention during past years. For the sludge processing, some measures such as incineration, waste landfill and composting, are generally used. In all these methods, sludge drying is often a necessary step due to several reasons. Firstly, drying can largely reduce the water content and result in large mass and volume reduction of sludge, which leads to a cost reduction in transport, handling and storage. Secondly, drying at high temperature can kill many pathogen germs and stabilize sludge systems to some extend. Thirdly, the removal of water will increase the calorific value of the sludge, which can be used as acceptable combustible sources.

Significant economic, industrial and environmental interests have provided incentives for the study of sludge drying in recent years [3–19]. However, sludge is itself a complicated heterogeneous mixture of microorganisms, mineral particles, multiphase flow structures and organic polymers, and the composition varies considerably. During the drying process, two or three phase flow pattern prevails within sludge systems. Internal dynamic behavior of sludge during the drying process may vary from one sample to another significantly. Due to such a complexity, the researches in open literature were largely focused on specific industrial applications and phenomenal aspects on the sludge drying. The prediction of the drying rate remained principally an empirical art and little emphasis was paid to the mechanistic field within a dried sludge. It is apparent that internal microscopic dynamic processes of sludge drying systems are responsible for the macroscopic drying behaviors. A profound mechanistic study of internal dynamics of dried sludge can therefore provide grounded evidence for phenomenal results and guide industrial applications.

Dried sludge systems live far from the equilibrium state and their internal dynamics are significantly different from the classical equilibrium phenomenon. The difficult factors include the random distribution of compositions within the sludge, the growth and evolution of clusters, the variable permeability and the complex multiphase flow patterns. All these can induce complicated structures far from equilibrium inside the dried sludge. In principle, all of these difficulties can be rationally overcome if the nonlinear controlling equations of dried sludge can be solved. However, the physical foundation of dealing with

* Tel.: +86 22 27890550; fax: +86 22 87402076.
E-mail address: lhchai@tju.edu.cn.

1290-0729/$ – see front matter
doi:10.1016/j.ijthermalsci.2006.10.011

Nomenclature

c	constant	$\sigma, \bar{\sigma}$	constants
$f_1, \ldots, f_4$	constants	ε	constant defined in Eq. (25)
F_u, F_s	fluctuation forces introduced in Eqs. (14) and (15)	η	constants
h	flux transfer coefficient ..... $\mathrm{J\,m^{-2}\,K^{-1}}$	λ	constants
$J, \bar{J}$	flux ..... W	α	controlling parameter appeared in Eq. (16)
J''	flux density ..... $\mathrm{W\,m^{-2}}$	α, β	constants
l	scale	γ	constants
p	index defined in Eq. (22)	$\Phi, \bar{\Phi}$	potential functions
S	function defined in Eq. (14)	ψ	constant
t	time ..... s	ω	constant
T	function introduced in Eq. (15)	ζ	constant
u	velocity ..... $\mathrm{m\,s^{-1}}$	ξ	variables defined in Eq. (12), ... $\mathrm{K\,m^{-1}}$
x	driving force ..... $\mathrm{K\,m^{-1}}$	μ	constant
$\boldsymbol{x}$	driving force vector	Ω	area or volume unit
Greek symbols			
ρ	probability density		

these complicated nonlinear partial differential equations is not well established, and theoretical analyses on these equations are still difficult up to today.

To advance the mechanistic understanding of internal dynamics of sludge drying systems, a new perspective is highly needed. In this study, a new method from a statistical dynamic perspective was introduced to analyze the internal structural dynamics of sludge drying system. Fractal features and mechanisms of drying sludge were identified and a parametric study of some controlling conditions on fractal dimension of structures was conducted. Experimental studies were carried to validate the theoretical analysis and good agreements were found.

2. The theoretical framework on internal dynamics of sludge drying systems

2.1. Statistical dynamics of sludge drying systems

The multi-phase flow structures formation and evolution behavior are originated from and dependent on nonlinear dynamic interactions among small cells that constitute sludge systems. It is important to analyze structural characteristics from a microscopic view. As the cell number of multi-phase flow structures system is large and the nonlinear interactions among these cells are extraordinary complicated. An adequate dynamic description in most cases can only be achieved based on the statistical dynamics.

The primary distribution of multi-phase flow structures cells, or primary nodes of network, is shown in Fig. 1. For simplified analysis, each node is placed on a rectangle lattice. Assuming the driving forces of multi-phase flow structure cells, i.e., the cause of receiving flux from heating source, can be expressed as $x_1, x_2, \ldots x_n$, which are lumped as a vector $\mathbf{x} = (x_1, x_2, \ldots x_n)$. The driving forces here indicate temperature and/or concentration and/or pressure differences between multi-phase flow structure cells and the heating environment. Similar to the classical statistical mechanics theory, all possible microstates compose a continuous scope in the Γ space and $\mathrm{d}\mathbf{x} = \mathrm{d}x_1\mathrm{d}x_2\cdots\mathrm{d}x_n$ is a volumetric unit in Γ space. The probability for the state of a system existing within the volumetric unit $\mathrm{d}\mathbf{x}$ at time t is

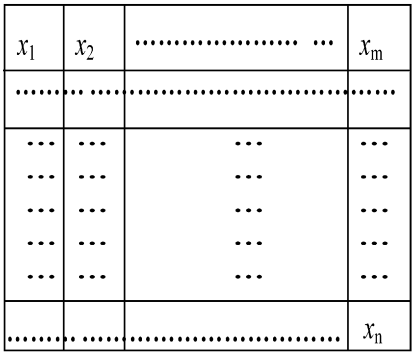

Fig. 1. An ensemble of interacting multi-phase flow structural cells.

$$\rho(\mathbf{x}, t)\,\mathrm{d}\mathbf{x} \tag{1}$$

where $\rho(\mathbf{x}, t)$ is distribution function of ensemble and satisfies the normalization condition

$$\int \rho(\mathbf{x}, t)\,\mathrm{d}\mathbf{x} = 1 \tag{2}$$

Assuming that the flux induced by multi-phase flow structure cells is J when the state of the system exists within the volumetric unit $\mathrm{d}\mathbf{x}$ at the time t, the averaged flux over all possible microstates is

$$\bar{J} = \int \rho(\mathbf{x}, t) J(\rho)\,\mathrm{d}\mathbf{x} \tag{3}$$

The flux can be seen as generated from coupled interactions among cells. Thus, J can be written as:

$$J = \eta + \sum_i \gamma_i x_i + \sum_{ij} \gamma_{ij} x_i x_j + \sum_{ijk} \gamma_{ijk} x_i x_j x_k$$

$$+\sum_{ijkl}\gamma_{ijkl}x_i x_j x_k x_l+\cdots \tag{4}$$

By use of Lagrange multiplier, let us maximize Eq. (3) under the below constraints (i.e., given prices) in Eq. (5), which stands for mass or energy conservations

$$\langle x_i\rangle = f_1,\quad \langle x_i x_j\rangle = f_2,\quad \langle x_i x_j x_k\rangle = f_3,\quad \langle x_i x_j x_k x_l\rangle = f_4 \tag{5}$$

We obtain that

$$J=\alpha+\sum_i \beta_i x_i+\sum_{ij}\beta_{ij}x_i x_j+\sum_{ijk}\beta_{ijk}x_i x_j x_k +\sum_{ijkl}\beta_{ijkl}x_i x_j x_k x_l+\frac{c}{\rho} \tag{6}$$

Where c is integration constant, and Eq. (6) can be changed as

$$\rho = c\Big/\left(J-\alpha-\sum_i\beta_i x_i-\sum_{ij}\beta_{ij}x_i x_j-\sum_{ijk}\beta_{ijk}x_i x_j x_k -\sum_{ijkl}\beta_{ijkl}x_i x_j x_k x_l\right) \tag{7}$$

Substituting Eq. (4) into Eq. (7) yields

$$\rho = c\Big/\left(\eta-\alpha+\sum_i(\gamma_i-\beta_i)x_i-\sum_{ij}(\gamma_{ij}-\beta_{ij})x_i x_j -\sum_{ijk}(\gamma_{ijk}-\beta_{ijk})x_i x_j x_k -\sum_{ijkl}(\gamma_{ijkl}-\beta_{ijkl})x_i x_j x_k x_l+\cdots\right) \tag{8}$$

As it is known that

$$\mathrm{e}^x = 1+x+\frac{1}{2!}x^2+\frac{1}{3!}x^3+\cdots \tag{9}$$

We obtain that [20,21]

$$\rho=\exp\left(\mu+\sum_i\sigma_i x_i+\sum_{ij}\sigma_{ij}x_i x_j+\sum_{ijk}\sigma_{ijk}x_i x_j x_k +\sum_{ijkl}\sigma_{ijkl}x_i x_j x_k x_l+\cdots\right) \tag{10}$$

The exponential term of Eq. (8) can be defined as the potential function [20,21]

$$\Phi(\sigma,x)=\mu+\sum_i\sigma_i x_i+\sum_{ij}\sigma_{ij}x_i x_j+\sum_{ijk}\sigma_{ijk}x_i x_j x_k +\sum_{ijkl}\sigma_{ijkl}x_i x_j x_k x_l+\cdots \tag{11}$$

Where σ in left term represents a vector, and σ in right term represents a scalar. μ and σ are both parameters produced by Lagrange optimization, which are determined by parameters β and γ in Eq. (8). The potential function regulates all dynamic behaviors of interacting cell systems.

Accordingly, by transformation of

$$x_i=\sum_k\psi_{ki}\xi_k \quad\text{or}\quad \xi_i=\sum_k\omega_{ki}x_k \tag{12}$$

Eq. (11) can be changed as [20,21]

$$\bar{\Phi}(\lambda,\xi)=\zeta+\sum_k\lambda_k\xi_k^2+\cdots \tag{13}$$

By transformation of Eq. (12), ξ is to describe all the potential large-scaled patterns of multi-phase flow structures within the dried sludge as ξ is a linear combination of all cells expressed by x_k. Within dried sludge systems, ξ represents usually temperature and/or concentration and/or pressure differences between the heating environment and bulk multi-phase flow structural patterns. Apparently, ξ is also a dynamic variable for the patterns of multi-phase flow structures within dried sludge and it evolves during the whole drying process.

Inactive patterns ($\lambda_k<0$) represent multi-phase flow structures that will be eliminated and cannot survive to form, and the active patterns ($\lambda_k>0$) stand for survival and formation of multi-phase flow structures. In other words, the multi-phase flow structures (or flow channels for more visualization) within the dried sludge is largely dependent on the parameter λ. From the above analysis, it is clear that λ in Eq. (13) or σ in Eq. (11) and ω in Eq. (12) are decided by the parameters β and γ in Eq. (8). While β and γ have a tight relationship with operational parameters, at least in principle. As a consequence, the above novel theoretical framework bridges the gap between operational conditions and the dynamic evolution of multi-phase flow structures within sludge drying systems. Such a variational method makes the constraint conditions that once difficult to be tackled due to complicated nonlinear interactions become easier to be dealt with. The focus of this work is the dynamic evolution of multi-phase flow structures within sludge drying systems. It would be helpful to be noted that the effects of external transfers between the sludge sample and the surrounding atmosphere, which largely depend on parameters of the air and can significantly affect the drying kinetics, can be included in parameters β and γ of the theoretical framework, at least in principle.

In order to further reveal the evolving dynamics of multi-phase flow structures within sludge drying systems, the following two groups of Langevin equations can be obtained from Eq. (13)

$$\dot{\xi}_u=\lambda_u\xi_u+S_u(\xi_u,\xi_s)+F_u(t),\quad \lambda_u>0 \tag{14}$$

$$\dot{\xi}_s=\lambda_s\xi_s+T_s(\xi_u)+F_s(t),\quad \lambda_s<0 \tag{15}$$

According to the equation, it is clear that parameter λ is actually a kind of damping coefficient. Through a series of analyses [20], it was found that the flux change close to the instability point is only governed by the patterns with $\lambda_u>0$ (small damping coefficient), i.e.

$$\bar{J}(\alpha_1)-\bar{J}(\alpha_2)\approx J_u(\alpha_1)-J_u(\alpha_2) \tag{16}$$

Eq. (16) provides a vivid physical dynamic picture within dried sludge systems. Only active patterns of multi-phase flow structures with stronger ability can acquire more flux and grow.

Although many potential patterns may exist in an open complex multi-phase flow structure systems, only some of them can use the input of flux better. Flux is therefore concentrated in one or a few patterns, which then dominate the macroscopic behavior of the whole system. Multi-phase flow structures formation is therefore a self-organized dynamic process and the resultant multi-phase flow structures are typical ordered dissipative structures. The self-organized analysis provides useful information to understand the formation of the ordered dissipative structure. The above analyses illustrates that the heterogeneous multi-phase flow structures can occur spontaneously (without any supposition on influence of the cells directly). The self-organized formation of multi-phase flow structures can be rationalized in a sound way. Further analysis of the heterogeneous multi-phase flow structures within dried sludge is conducted in below sections.

2.2. Formations of hierarchical multi-phase flow structures within dried sludge

The above analyses shed new light on the multi-phase flow structure patterns formation qualitatively. Multi-phase flow structures usually show variable hierarchical features depending on specific operational conditions. To describe the hierarchical structures quantitatively, a rectangle area was selected as shown in Fig. 2(a). A physical picture on the growth of a typical micro-volume of multi-phase flow structures within dried sludge can be analyzed as below. The multi-phase flow structure continues to spread through the interactions (such as impulsion, adsorption of or collision) with other structural cells with increasing time and scale. A multi-phase flow structure of scale l is shown in Fig. 2(b), which is an enlarged illustration of rectangle area shown in Fig. 2(a). The term dl represents the infinite scale increment from scale l to scale $l + \mathrm{d}l$. The vertical axis represents the direction of structures growing, and the curve represents the development of a boundary layer. The term u and ξ represents the velocity distribution and the concentration distribution of flux induced by multi-phase flow structures .The adjacent structural cells diffuse from the bulk into the multi-phase flow structure through a boundary layer, within which the cells are continuously adsorbed and converted to the part of multi-phase flow structures. Therefore, the multi-phase flow structures will grow in scale and the boundary layer will thicken accordingly.

Taking into consideration of the energy conservation between the two adjacent scales, as showed in Fig. 2(b), the following series of equations can be obtained. The flux input per unit time from the dried sludge bulk to the growing multi-phase flow structure through the interface 3–4 is

$$\mathrm{d}l\frac{\mathrm{d}}{\mathrm{d}l}\int_0^l \xi_s u\,\mathrm{d}y \tag{17}$$

The flux output per unit time through the interface 1–2 is

$$-a\,\mathrm{d}l\left(\frac{\partial \xi}{\partial y}\right)\bigg|_w \tag{18}$$

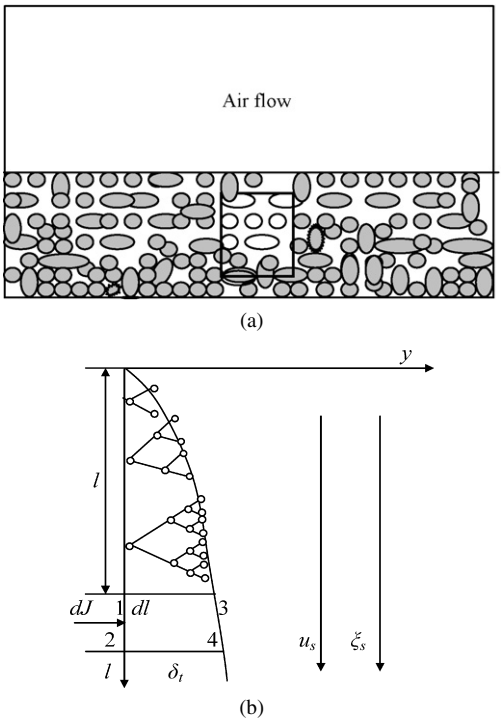

Fig. 2. (a) An illustration of multi-phase flow structures within dried sludge. (b) An illustration of enlarged part of selected part in (a).

The flux increase per unit time along scale increment through the interface 1–3 and 2–4 is

$$\mathrm{d}l\frac{\mathrm{d}}{\mathrm{d}l}\int_0^l \xi u\,\mathrm{d}y \tag{19}$$

According to the cascade flux balance

$$\mathrm{d}l\frac{\mathrm{d}}{\mathrm{d}l}\int_0^l \xi_s u\,\mathrm{d}y - \mathrm{d}l\frac{\mathrm{d}}{\mathrm{d}l}\int_0^l \xi u\,\mathrm{d}y - a\,\mathrm{d}l\left(\frac{\partial \xi}{\partial y}\right)\bigg|_w = 0 \tag{20}$$

The flux conservation equation for growing multi-phase flow structure can be obtained

$$\xi_s\frac{\mathrm{d}}{\mathrm{d}l}\int_0^l u\,\mathrm{d}y - a\left(\frac{\partial \xi}{\partial y}\right)\bigg|_w = \frac{\mathrm{d}}{\mathrm{d}l}\int_0^l \xi u\,\mathrm{d}y \tag{21}$$

For arbitrary u and ξ distributions, Eq. (21) usually yields flux transfer coefficient as:

$$h = \frac{\partial \xi}{\partial y}\bigg|_{y=0} \sim l^{-p} \tag{22}$$

Depending on actual distributions of u and ξ, p is a specific parameter ranging from 0 to 1. Let h_n be the cell flux transfer coefficient at n-level, thus the flux transferred into the multi-phase flow structures can be described as:

$$\Omega_n \Delta J'' = h_n l^D \xi_n \tag{23}$$

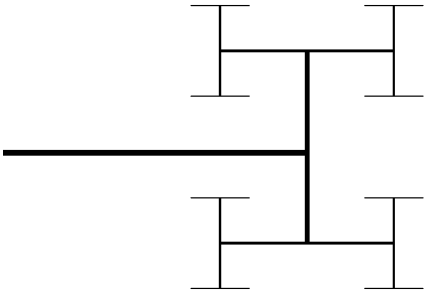

Fig. 3. An illustration of self-similar multi-phase flow structures.

Assuming that the structures formed in the same bulk conditions, we obtain from Eq. (23) (with $D = 2$)

$$\frac{\Omega_n \Delta J''}{\Omega_{(n-1)} \Delta J''} = \frac{h_n l_n^2 \xi_n}{h_{(n-1)} l_{(n-1)}^2 \xi_{n-1}} \sim \left[\frac{l_n}{l_{(n-1)}}\right]^{(2-p)} \tag{24}$$

Eq. (24) quantitatively expresses a typical fractal structure, as shown in Fig. 3, which may stand for hierarchical multi-phase flow structures within dried sludge.

The parameter $2-p$ is the fractal dimension and its value indicates the distribution feature of multi-phase flow structures. Let us here consider the solutions of Eq. (21) under some typical situations [21–23]. If u and ξ have trivial polynomial distribution (c_2), which may correspond to case of laminar flux transfer, we have $p = 0.5$ and $2-p = 1.5$. If u and ξ have exponential distribution (c_3), which may correspond to the case of turbulent flux transfer, we have $p = 0.2$ and $2-p = 1.8$; if u and ξ have trivial linear distribution (c_1), which may correspond to sole solid particles conductive flux transfer, we have $p = 1$ and $2-p = 1$ (it is no surprise that no fractal structures will form in this case). If u and ξ have almost uniform distribution (of course it is an ideal case), which may correspond to extremely turbulent flux transfer, we have $p = 0$ and $2-p = 2$ (it is natural that solid 2D Euclidean structures will form in this case).

The above analyses are based on some typical u and ξ distributions, which correspond to ideal flux transfer situations. For non-typical cases, the generalized flux can be considered as a hybrid of the two types of ideal flux transfer. The flux can be assumed to comprise a fraction β of the flux that is related to the index p_1, and the fraction $1-\beta$ of the flux that is related to the index p_2, where p_1 and p_2 are the two extreme points of the two ideal flux transfer situations. Based on the conservation of the generalized flux,

$$l^{-p} = \beta l^{-p_1} + (1-\beta) l^{-p_2} \tag{25}$$

where β is related to operational factors of the system, essentially reflecting and regulating the actual distribution of u and ξ. Therefore, β is actually an parameter that can reflect all type of the flux patterns and the distributions of u and ξ. From Eq. (25), we can derive the equation as follows

$$p = -\frac{\ln(\beta l^{-p_1} + (1-\beta) l^{-p_2})}{\ln l} \tag{26}$$

It is apparently that there will be different p values and multi-phase flow structures for different u and ξ distributions. Logical conclusions could be drawn that under high heating flux conditions, multi-phase flow within dried sludge is very intense and is similar to the strong turbulent flow. A high density (i.e., high fractal dimension) of multi-phase flow structures may be formed. Under low heating flux conditions, multi-phase flow within dried sludge is less intense than the violent turbulent, a low density (i.e., low fractal dimension) of multi-phase flow structures may be formed. These results are qualitatively in agreement with experimental results.

2.3. Numerical calculations and connections to experimental measurements

The relationship among fractal dimension, scale and influence factor β can be revealed from Eq. (26) where the p_1 and p_2 represent values of p with different flow forms. When β have different values between 0 and 1, all possible combinations of typical flow forms can be obtained. Varied p values and fractal dimensions under various scales can be acquired from Eq. (26). Some typical values of p can be obtained: 0, 0.2, 0.5, and 1, which divide p value into 3 sections: [0, 0.2], [0.2, 0.5], [0.5, 1]. Different sections represent different flow forms. For example, values in the section [0.2, 0.5] indicate that the flux form is between turbulent flow and laminar flow, which are more common in nature. Figs. 4(a)–(c) represent how β influence $2-p$ under a certain scale. Fig. 5 represents relationship between $2-p$ and scale under a certain value of β. These figures indicate there are some sorts of relationship existed between fractal dimensions and scale even for similar β values.

Effects of all operational conditions on multi-phase flow structures within dried sludge can be expressed by parameters β and γ in Eq. (8), or σ in Eq. (11), or ω in Eq. (12) or λ in Eq. (13), or finally the distributions of u and ξ in Eq. (21). Doubtlessly, multi-phase flow structures will vary with shifts of operational conditions. The forgoing theoretical analyses may give a unified theoretical framework for the explanation of parametric effects on multi-phase flow structures within drying sludge systems. According to Fig. 4, once we measure the fractal dimension $2-p$ of the system or structure, we can obtain the profile of to understand internal dynamics of the system. Conversely, if the dynamic components interactions of the system under input flux were known, we can analytically derive the fractal dimension $2-p$. For example, in following experiments, by choosing a scale $l = 10^{-1}$ m, we can get the theoretical values of β and deduce the local flow forms (see Table 1).

After theoretically analyzing the internal dynamics with drying sludge systems, and revealing the fractal features of multi-phase flow structures, below sections will conduct experimental investigations to analyze the dynamic features of drying processes.

3. Experimental investigations on sludge drying systems

3.1. Materials and techniques

A sludge cake with a certain thickness fixed on a tank, whose surface is coated by a stainless mesh (40×40 mm), is hung on

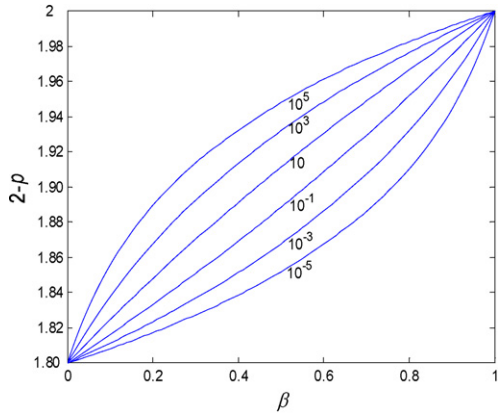

(a) $p = 0-0.2$

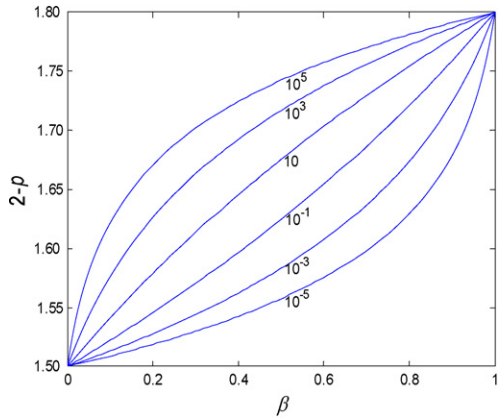

(b) $p = 0.2-0.5$

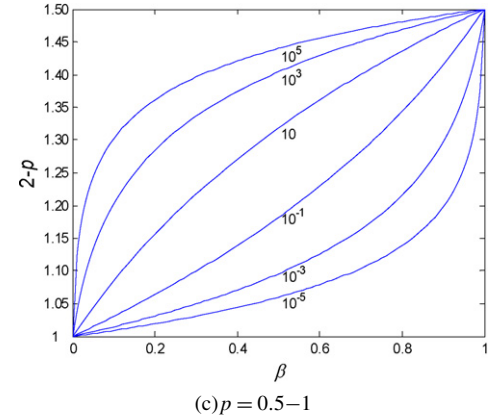

(c) $p = 0.5-1$

Fig. 4. The influence of β on the fractal dimension $2-p$, when p is between (a) 0–0.2; (b) 0.2–0.5;(c) 0.5–1, separately.

an electronic scale in a drying chamber. The electronic scale is connected by a computer to measure the mass of sludge on-line and thus to obtain the water evaporating rate. The schematic of the experimental set-up is shown in Fig. 6. Two kinds of drying methods are utilized.

(1) Heated wall contact drying

Power source is electronically adjusted to indirectly heat the sludge cake on a stain-plate underneath, as shown in Fig. 6(A). Three fans are used to maintain a certain amount of air flow. The parameters of air can be deduced by the atmospheric conditions. An electric field within sludge cake is produced by placing a DC

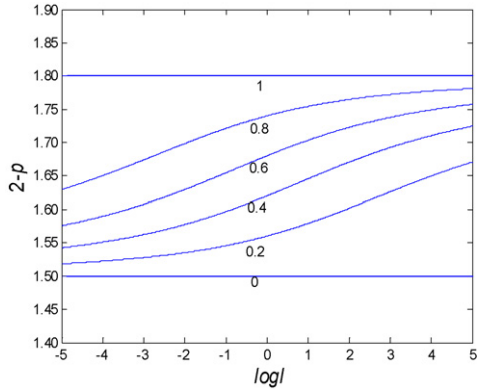

Fig. 5. The influence of the scale l on the fractal dimension $2-p$, when p is between 0.2–0.5.

power between stainless mesh and stain-plate for overcoming the wall adhesion.

Biological sludge is mainly composed of microorganisms, whose constitutive proteins are made of typical amopolyte-amino acids. Under conditions of pH=6.5, amopolyte is electronegative. Therefore, inside the sludge cake placed in the electric fields, electronegative microorganisms will move toward the anode, while hydrate molecules (say H_3O^+) run to the cathode. In our experiments, through inducing an electric field inside the sludge cake, in one way, the drying rate can be improved for the movement of hydrate molecules toward the cathode, in another way, technology problem of wall adhesion can be partially tackled for the movement of microorganisms toward the anode.

Raw sludge samples are collected from the sewage water treatment equipments in Tianjin University building 53. A 85%–87% aquiferous cylindrical sludge cake with diameter of 85 mm and thickness of 10 mm is then prepared by pretreatments such as simple condensations and dewatering (as conventional activated sludge process). The temperature at heating plate is about 110 °C, and air velocity is controlled at 0.45 m s^{-1}. Detailed parameters are outlined in Table 1.

(2) Infrared heating drying by incandescent bulbs (imitate solar radiations)

Four incandescent bulbs of 100 W are used to heat sludge to imitate the case of solar radiations. An electric field is also produced by placing a DC power between stainless mesh and stain-plate, as shown in Fig. 6(B). (Note: Fig. 6(A) and Fig. 6(B) are different only in heating methods and direction of electronic fields for comparisons.)

Raw sludge are collected from the sewage water treatment equipments in Ji Zhuang. Standard cylindrical sludge cake is 83%–84% aquiferous, with diameter of 85 mm and thickness of 10 mm or 20 mm. Water content of the sludge cakes at the end of the every experimental run can be obtained by measurement of the mass of sludge. The temperatures of air at entrance and exit are 20 °C and 33 °C respectively, and air velocity is controlled at 0.45 m s^{-1}. Detailed parameters are also outlined in Table 1.

Table 1
Experimental parameters and fractal dimensions of sludge drying systems

Groups	Heating methods	Sludge sample origins, types and sizes	Voltage	Index D	Fractal dimension $1+D$	Values of β in Eq. (26)	ξ distributions $\beta \times c_i + (1-\beta) \times c_{i+1}$
1	Heated wall contact drying (wall temperature 110 °C)	From building 53, Tianjin University, 85%, D85×10 mm	0	0.3265	1.3265	0.82	$0.82c_1 + 0.18c_2$
			5	0.3287	1.3287	0.83	$0.83c_1 + 0.17c_2$
			10	0.3617	1.3617	0.85	$0.85c_1 + 0.15c_2$
2	Heated wall contact drying (wall temperature 110 °C)	By self-trained, 87%, D85 ×10 mm	0	0.3703	1.3703	0.86	$0.86c_1 + 0.14c_2$
			5	0.5055	1.5055	0	c_3
			10	0.6119	1.6119	0.48	$0.48c_2 + 0.52c_3$
3	Infrared heating (imitating 45 °C solar radiation)	From Ji Zhuang, 83%, D85 ×10 mm	0	0.3347	1.3347	0.84	$0.84c_1 + 0.16c_2$
			5	0.3551	1.3551	0.85	$0.85c_1 + 0.15c_2$
			10	0.3794	1.3794	0.91	$0.91c_1 + 0.09c_2$
4	Infrared heating (imitating 45 °C solar radiation)	From Ji Zhuang, 83%, D85 ×20 mm	0	0.2572	1.2572	0.70	$0.70c_1 + 0.30c_2$
			5	0.3277	1.3277	0.83	$0.83c_1 + 0.17c_2$
			10	0.3338	1.3338	0.84	$0.84c_1 + 0.16c_2$

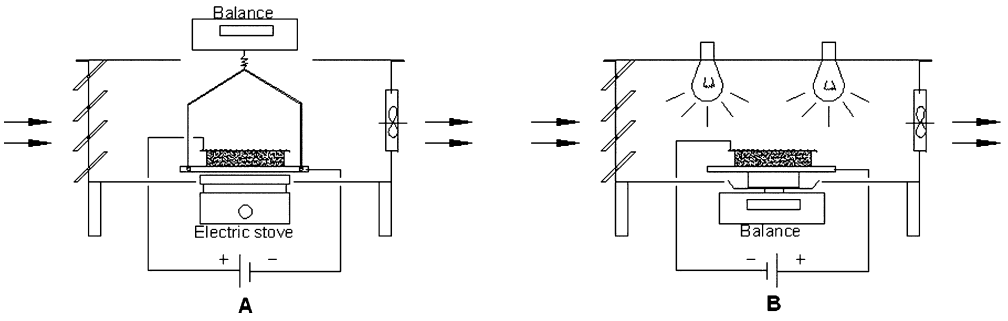

Fig. 6. Experimental apparatus (A: Heated wall contact drying; B: Infrared heating drying by incandescent bulbs).

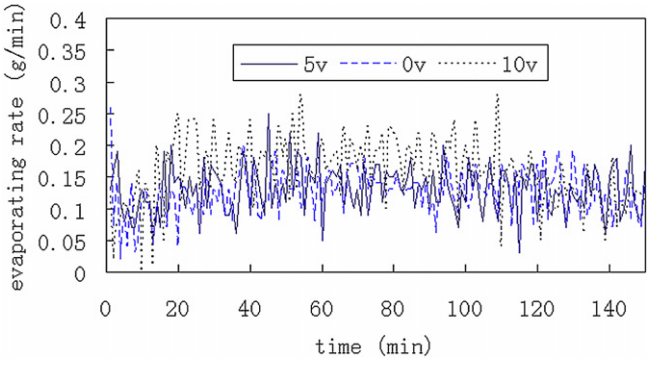

Fig. 7. Water evaporating rate of sludge cake drying (Group 1).

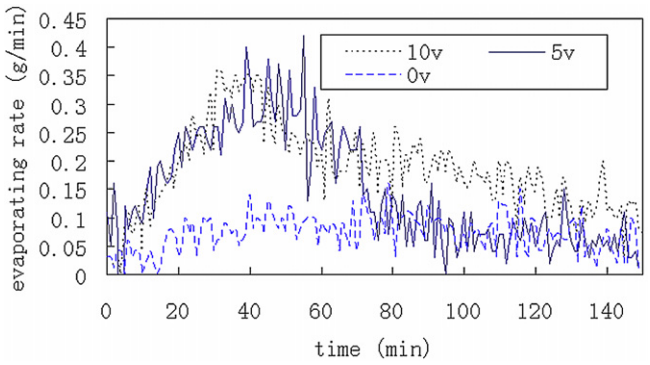

Fig. 8. Water evaporating rate of sludge cake drying (Group 2).

3.2. Experimental results and discussion

Four groups of experiments were conducted, whose controlling parameters were listed in Table 1. In each group, three runs of voltages were applied to obtain different curves of evaporating rates, as shown in Figs. 7–10.

In above theoretical sections, the fractal features of multiphase flow structures within dried sludge systems were analyzed. Though the shrinkage of sludge surface can be observed, it is difficult to directly get structural feature within sludge cake during drying. It is almost impossible to directly observe them by experiments. Fortunately, evaporating rate curve is closely related to the dynamic structures within sludge cake. A kind

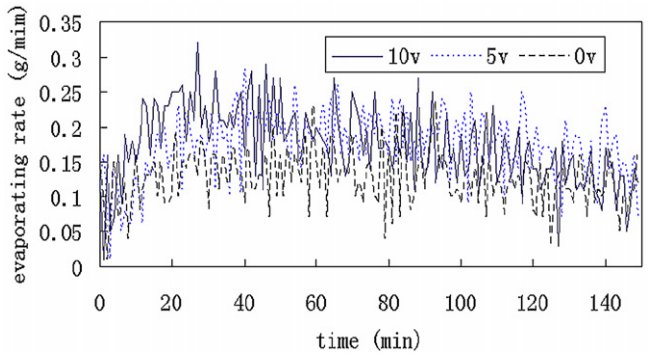

Fig. 9. Water evaporating rate of sludge cake drying (Group 3).

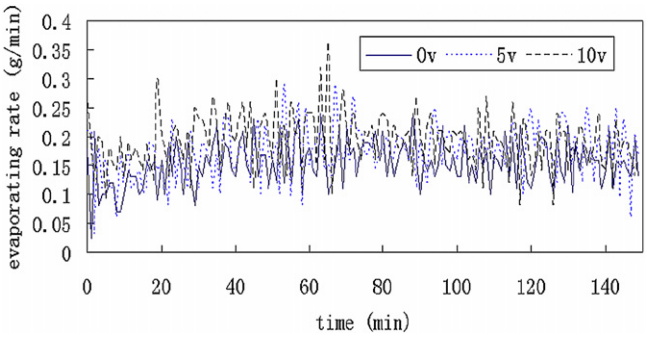

Fig. 10. Water evaporating rate of sludge cake drying (Group 4).

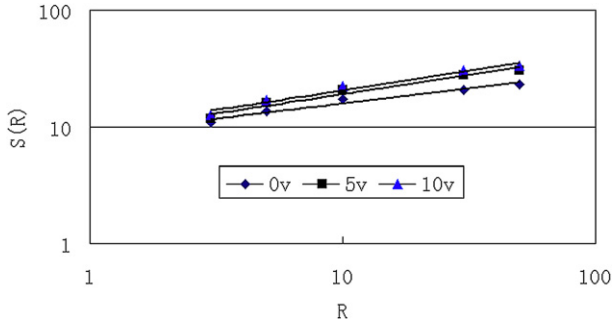

Fig. 11. Relationship of $S(R)$ and R (Group 1).

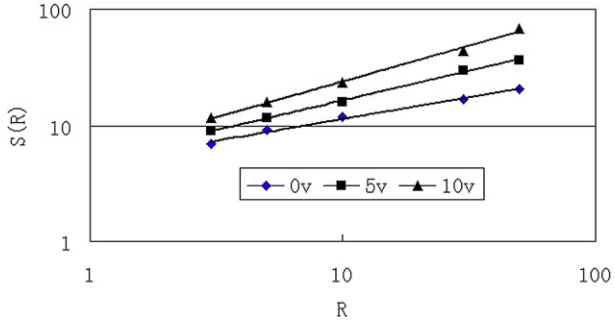

Fig. 12. Relationship of $S(R)$ and R (Group 2).

of fractal dimension in term of evaporating rate curves can be calculated as follows. We place a matrix box with width R to coat a segment of curve, and thus whose height equals the distance between crest and trough of chosen segment. By moving the box along the curve, the cumulative box area $S(R)$ can be calculated. By varying R, different $S(R)$ can be obtained. The tendency curve of $\log S(R) \sim \log R$ as in Figs. 11–14 are obtained, whose slopes are D. Corresponding fractal dimension is obtained as $1+D$ for two-dimensional cases. Table 1 shows the fractal dimensions calculated in term of evaporating rate curves in the controlled experiments. It is no surprise that our experimental results surely show fractal features. Keeping foregoing theoretical results in mind, we may confidently conclude that fractal features of dried sludge system were confirmed by both experiments and theories.

Though it has not yet been confirmed whether fractal dimension $1+D$ obtained from the evaporating rate curves is exactly equivalent to the fractal dimension $2-p$ of multi-phase flow structures within dried sludge systems, their positive correla-

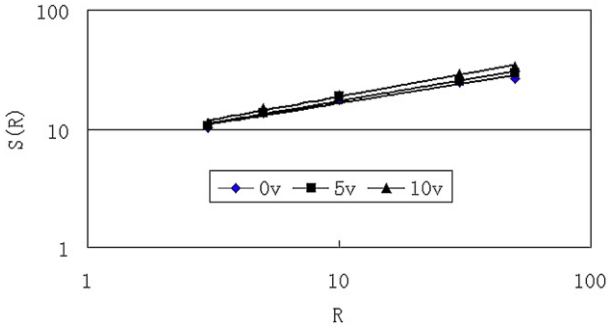

Fig. 13. Relationship of $S(R)$ and R (Group 3).

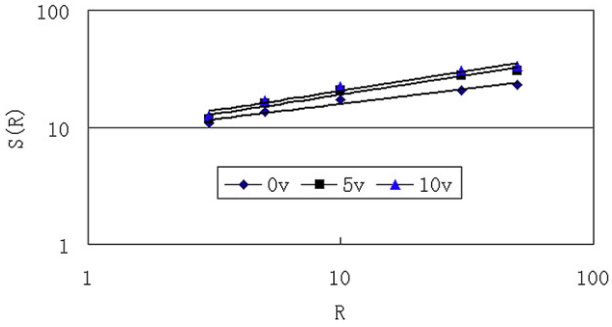

Fig. 14. Relationship of $S(R)$ and R (Group 4).

tions are strong. So the mechanistic analyses on experimental results can be conducted based on theoretical dynamic perspectives. This significantly contrasts to previous open studies where the fractal phenomena and dimension of multi-phase flow structures in sludge drying process was often neglected. Such a relationship is confirmed both experimentally and analytically in this study. The multi-phase flow inside sludge cake during drying processes have self-similar structures and the fractal dimension can be considered as a useful guide to understand the dynamics of sludge drying and effects of operational parameters.

The factors influencing the structure of sludge drying may be classified into the intrinsic and extrinsic factors. In the proposed new framework, these parametric factors may often be included into the u and ξ distributions. Distributions of u and ξ(corresponding structural index p) largely depend on these intrinsic and extrinsic factors. If the changes of these extrinsic and intrinsic factors are beneficial for the flux transfer, the p value will decrease and fractal dimension $2-p$ will increase. Experimental results on fractal dimensions as shown in Table 1 partially support this fact. Furthermore, in terms of above analyses, based on fractal dimension and operational conditions, we can analytically conjecture the u and ξ distributions, as shown in Table 1.

Fractal features shown by Table 1 reveals some subtle information, as analyzed below focusing on the four aspects: voltage, sample origin, heating method and size effect.

Firstly, very different features are found for the fractal dimensions under different voltages conditions. In general, the larger the voltages, the larger the fractal dimensions will be. In all groups of experiments, same tendencies are found. Accord-

ing to the theoretical framework, this is because the more internal active points (with $\lambda_k > 0$) of multi-phase flow structures will be activated with increasing voltages. More available active points will result in more intensive multi-phase flow within dried sludge, so the fractal dimension increases with increasing voltages. However, compared to other groups, data of the second group in the controlled experiments show the largest increases. According to the theoretical framework, this can be attributed to the fact that the higher water content is beneficial for increasing active points and multi-phase flow intensity compared to other groups of experiments. So the fractal dimension increases larger than those under other conditions.

Secondly, effects of sample origins of sludge (with different compositions and water content) on fractal dimensions are also significant. In the experiments, three types of sample origins were used, as shown in Table 1. Up to today, it is still difficulty to correlate the effects of sludge sample origin on its drying behavior (fractal dimensions) for its compositive complexity, for example, in terms of volatile fraction and exopolymer concentration. However, according to the theoretical framework, it is out of question to draw the conclusion that sludge drying with more intensive flow pattern has larger fractal dimensions. Compared to other groups, group 2 has larger fractal dimensions. Slight differences in fractal dimensions also exist among other three groups. This phenomenon can be described by Eq. (21). It is the different compositions of sludge that leads to the different distributions of u and ξ and thus different fractal dimensions. For example, some conditions such as the availability ratio of the adsorption point in the multi-phase flow structures have surely been a bit different during the drying process, which induced the slightly varied internal multi-phase flow structures. Therefore, it is no surprise that the fractal dimension will be different for different sample origins of sludge.

Thirdly, heating methods affect drying features too. In the experiments, it is evidently that the fractal dimensions for heated wall contact drying are higher than that of infrared heating. Based on the above discussions and theoretical analyses, the phenomenon can be understood from a new insight. In the experiments, the flux input into multi-phase flow structures is higher for heated wall contact drying than for infrared heating, thus the distributions of u and ξ is more intensive, which results in the higher fractal dimensions under heated wall contact drying. However, it is difficult to accurately discuss the impact of the kind of heating methods for the supplied power per mass unit of sample is not the same in all the experiments. Suitable drying method should be chosen in relation to variable sludge quantities.

Lastly, comparing group 3 with group 4, it is evidently that the fractal dimensions for small size of sludge are higher than those for large size. Based on the theoretical insights, the phenomenon can be understood from a new perspective. According to theoretical discussions, the attraction of multi-phase flow structures to adjacent cells will decrease with the increase of size. Moreover, the internal channels for large size are always easier to be counterchecked by the exterior branches. All of these factors are responsible for higher flux input into multi-phase flow structures for small size than for large size. The more intensive distributions of u and ξ, leading higher fractal dimensions is therefore expected. Of course, the present results are preliminary. It is more accurate to assess the effect of size according to the surface area per volume of the sludge cake in the further experiments.

In a word, the present analytical results are qualitatively in good agreement with experimental phenomena and may provide good instructions for industrial applications such as on how to enhance sludge drying rate. However, for sludge drying is a rather complicated problem, there remain lots of unsolved issues. The present paper provides a preliminary mechanistic investigation on sludge drying systems, and would act as catalysis for further investigations and provide some guidance for future industrial applications.

4. Conclusions

The formation and dynamic evolution of multi-phase flow structures within dried sludge is a challenged issue to researchers during recent years. This paper proposed a novel theoretical statistical dynamic analysis on the interactions among multi-phase flow structures cells within dried sludge and their environments. The fractal dimension of a drying heterogeneous structure was derived analytically and its relationship with some controlling factors was analyzed. The experiment results were exhibited to logically explain the novel theoretical framework. The present investigations, although preliminary, made a renewed theoretical effort to understand the underlying mechanisms of multi-phase flow structures cells nonlinear interactions among within sludge drying systems. The present studies may not only give more rational and mechanistic descriptions on sludge drying systems, but would be promising for industrial implications.

Acknowledgements

The Project is currently sponsored by National Natural Science Foundation of China through the Contract #50406018 and the Scientific Research Foundation for the Returned Overseas Chinese Scholars. Experimental help from Dr. Ma is highly appreciated. Suggestions from anonymous reviews and a detailed polish on language by Dr. Wen in Leeds University are sincerely thanked.

References

[1] P. Brautlecht, S. Gredigk, Concept for an interlinked system of a sludge drying facility and a landfill for residual waste, Water Science and Technology 38 (2) (1998) 119–125.
[2] U. Luboschik, Solar sludge drying – based on the IST process, Renewable Energy 16 (1–4) (1999) 785–788.
[3] S. Nielsen, N. Willoughby, Sludge treatment and drying reed bed systems in Denmark, Water and Environment Journal 19 (4) (2005) 296–305.
[4] A. Idris, O.B. Yen, M.H. Hamid, A.M. Baki, Drying kinetics and stabilization of sewage sludge in lagoon in hot climate, Water Science and Technology 46 (9) (2002) 279–286.
[5] P. Arlabosse, S. Chavez, C. Prevot, Drying of municipal sewage sludge: From a laboratory scale batch indirect dryer to the paddle dryer, Brazilian Journal of Chemical Engineering 22 (2) (2005) 227–232.

[6] B. Wett, M. Demattio, W. Becker, Parameter investigation for decentralised dewatering and solar thermic drying of sludge, Water Science and Technology 51 (10) (2005) 65–73.
[7] P. Cooper, N. Willoughby, D. Cooper, The use of reed-beds for sludge drying, Water and Environment Journal 18 (2) (2004) 85–89.
[8] A. Reyes, M. Eckholt, F. Troncoso, et al., Drying kinetics sludge from a wastewater treatment plant, Drying Technology 22 (9) (2004) 2135–2150.
[9] T. Tao, X.F. Peng, D.J. Lee, Thermal drying of wastewater sludge: Change in drying area owing to volume shrinkage and crack development, Drying Technology 23 (3) (2005) 669–682.
[10] A. Leonard, S. Blacher, P. Marchot, et al., Convective drying of wastewater sludges: Influence of air temperature, superficial velocity, and humidity on the kinetics, Drying Technology 23 (8) (2005) 1667–1679.
[11] A. Leonard, P. Vandevenne, T. Salmon, et al., Wastewater sludge convective drying: Influence of sludge origin, Environmental Technology 25 (9) (2004) 1051–1057.
[12] J. Vaxelaire, J.R. Puiggali, Analysis of the drying of residual sludge: From the experiment to the simulation of a belt dryer, Drying Technology 20 (4–5) (2002) 989–1008.
[13] J.B. Chen, X.F. Peng, T. Tao, et al., Thermal drying of wastewater sludge with crack formation, Water Science and Technology 50 (9) (2004) 177–182.
[14] S. Al-Muzaini, Performance of sand drying beds for sludge dewatering, Arabian Journal for Science and Engineering 28 (2B) (2003) 161–169.
[15] M. Yamaoka, K. Hata, Improvements in drying beds for non-concentrated sludge, Advances in Environmental Research 7 (3) (2003) 721–725.
[16] M. Bux, R. Baumann, S. Quadt, et al., Volume reduction and biological stabilization of sludge in small sewage plants by solar drying, Drying Technology 20 (4–5) (2002) 829–837.
[17] Y.S. Shin, H.C. Kim, H.S. Chun, Drying of water treatment process sludge in a fluidized bed dryer, Korean Journal of Chemical Engineering 17 (1) (2000) 22–26.
[18] G.H. Chen, P.L. Yue, A.S. Mujumdar, Sludge dewatering and drying, Drying Technology 20 (4–5) (2002) 883–916.
[19] J. Vaxelaire, J.M. Bongiovanni, J.R. Puiggali, Mechanical dewatering and thermal drying of residual sludge, Environmental Technology 20 (1) (1999) 29–36.
[20] L.H. Chai, M. Shoji, Self-organization and self-similarity in boiling systems, ASME Journal of Heat Transfer 124 (3) (2002) 507–515.
[21] H. Haken, Information and Self-Organization, Springer, Berlin, 2000.
[22] L.H. Chai, D.S. Wen, Hierarchical self-organization of complex systems, Chemical Research in Chinese Universities 20 (4) (2004) 440–445.
[23] L.H. Chai, A theoretical analysis of bubble interaction in boiling systems, International Journal of Thermal Science 43 (11) (2004) 1067–1073.